Photoinduced Reduction of Manganese(III) meso-Tetrakis(1-methylpyridinium-4-yl)porphyrin at AT and GC Base Pairs

ARTICLE *in* THE JOURNAL OF PHYSICAL CHEMISTRY B · JULY 2013

Impact Factor: 3.3 · DOI: 10.1021/jp4027699 · Source: PubMed

8 AUTHORS, INCLUDING:

S.-D. Jung
Electronics and Telecommunications Researc…
49 PUBLICATIONS **1,419** CITATIONS
SEE PROFILE

Chan Im
Konkuk University
77 PUBLICATIONS **810** CITATIONS
SEE PROFILE

Seog K Kim
Yeungnam University
93 PUBLICATIONS **1,209** CITATIONS
SEE PROFILE

Dae Won Cho
Korea University
106 PUBLICATIONS **1,405** CITATIONS
SEE PROFILE

THE JOURNAL OF PHYSICAL CHEMISTRY B

Article

pubs.acs.org/JPCB

Photoinduced Reduction of Manganese(III) *meso*-Tetrakis(1-methylpyridinium-4-yl)porphyrin at AT and GC Base Pairs

Yong Hee Kim,[†] Sang Don Jung,[†] Myoung Hee Lee,[‡] Chan Im,[‡] Yun-Hwa Kim,[§] Yoon Jung Jang,[§] Seog K. Kim,*[,§] and Dae Won Cho*[,¶]

[†]BT Convergence Technology Research Department, ETRI, Daejeon 305-700, Korea

[‡]Konkuk University-Fraunhofer ISE Next Generation Solar Cell Research Center, Konkuk University, Seoul 143-701, Korea

[§]Department of Chemistry, Yeungnam University, Gyeongsan City, Gyeong-buk 712-749, Korea

[¶]Department of Advanced Materials Chemistry, 2511 Sejong, Korea University, Sejong 339-700, Korea

Supporting Information

ABSTRACT: The photoreduction of water-soluble cationic manganese(III) *meso*-tetrakis(1-methylpyridium-4-yl)porphyrin ($Mn^{III}(TMPyP)^{4+}$) bound to a synthetic polynucleotide, either poly[d(A-T)$_2$] or poly[d(G-C)$_2$], was examined by conventional absorption and circular dichroism (CD) spectroscopy, transient absorption, and transient Raman spectroscopy. Upon binding, $Mn^{III}(TMPyP)^{4+}$ produced a positive CD signal for both polynucleotides, suggesting external binding. In the poly[d(A-T)$_2$]−$Mn^{III}(TMPyP)^{4+}$ adduct case, an interaction between the bound porphyrin was suggested. The transient absorption spectral features of $Mn^{III}(TMPyP)^{4+}$ in the presence of poly[d(A-T)$_2$] and poly[d(G-C)$_2$] were similar to those of the photoreduced products, $Mn^{II}(TMPyP)^{4+}$, whereas $Mn^{III}(TMPyP)^{4+}$ in the absence of polynucleotides retained its oxidation state. This indicated that both poly[d(A-T)$_2$] and poly[d(G-C)$_2$] act as electron donors, resulting in photo-oxidized G and A bases. The transient Raman bands (ν_2 and ν_4) that were assigned to porphyrin macrocycles exhibited a large downshift of ~25 cm^{-1}, indicating the photoreduction of Mn^{III} to Mn^{II} porphyrins when bound to both polynucleotides. The transient Raman bands for pyridine were enhanced significantly, suggesting that the rotation of peripheral groups for binding with polynucleotides is the major change in the geometry expected in the photoreduction process. These photoinduced changes do not appear to be affected by the binding mode of porphyrin.

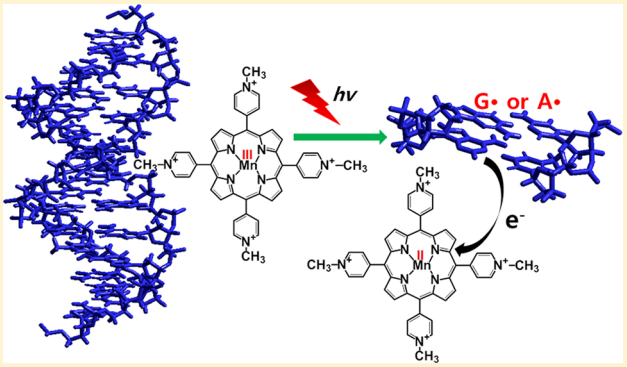

INTRODUCTION

Irreversible DNA damage and nucleobase modification after exposure to light are the major research subjects in the fields of aging,[1] inflammatory disease,[2] and carcinogenesis.[3] One of the purine bases, guanine (G), is considered to be the site with the lowest ionization potential in DNA, acting as a hole-transfer medium in long-range electron-transfer reactions.[4,5] Guanine is oxidized to the intermediate radical cation $G^{\bullet+}$, which gives rise to permanent lesions that enable sequence-specific DNA strand scissions.[6] The active areas of current research are the photoinduced formation of $G^{\bullet+}$ and the development of synthetic nucleic acid cleavage agents that can be controlled by light.[7] Therefore, additional interest has been focused on the selectivity of photoreceptor molecules for the binding sites because the binding patterns with DNA affect the photochemical mechanisms and direct interactions.

The interactions of porphyrin derivatives with DNA have been interesting subjects of many investigations since the pioneering work of Fiel[8,9] and Pasternack and co-workers.[10−12] Water-soluble porphyrins are excellent probes for monitoring the structure and dynamics of nucleic acids and proteins. In addition to use as probe, porphyrins have also attracted attention for medical applications, such as suppression of the HIV-1 virus responsible for AIDS[13] and photodynamic therapy (PDT).[14] Therefore, the interaction of water-soluble free-base *meso*-tetrakis(1-methylpyridinium-4-yl)porphyrins ($TMPyP^{4+}$), which is a representative of the porphyrin family, and their metallo-derivatives ($M\text{-}TMPyP^{4+}$) have been studied extensively using NMR,[15−17] steady-state and time-resolved fluorescence,[18] circular (CD) and linear dichroism dichroism (LD),[19−23] and time-resolved resonance Raman techniques.[24,25]

Manganese(III) porphyrins are classified as d-type hypercomplexes.[26] A paramagnetic d^4 metal, manganese(III) has a vacancy in the $e_g(d_\pi)$ orbitals, which enables a porphyrin ligand-to-metal charge-transfer transition.[27] The relatively low metal redox potentials of manganese(III) porphyrins enables their use in variety of photoreactions. In this study, the photoreduction

Received: March 20, 2013
Revised: July 10, 2013
Published: July 30, 2013

dx.doi.org/10.1021/jp4027699 | *J. Phys. Chem. B* 2013, 117, 9585−9590

of cationic $Mn^{III}(TMPyP)^{4+}$ (Scheme 1) bound to poly[d(A-T)$_2$] and poly[d(G-C)$_2$] was examined by transient absorption and transient resonance Raman (RR) measurements. The binding mode of $Mn^{III}(TMPyP)^{4+}$ to native DNA was recently reported.[20] Based on the reported binding mode of the $Mn^{III}(TMPyP)^{4+}$–DNA complex, those of the $Mn^{III}(TMPyP)^{4+}$-poly[d(A-T)$_2$] and -poly[d(G-C)$_2$] adducts were also examined using the CD spectrum.

Scheme 1. Chemical Structure of $Mn^{III}(TMPyP)^{4+}$

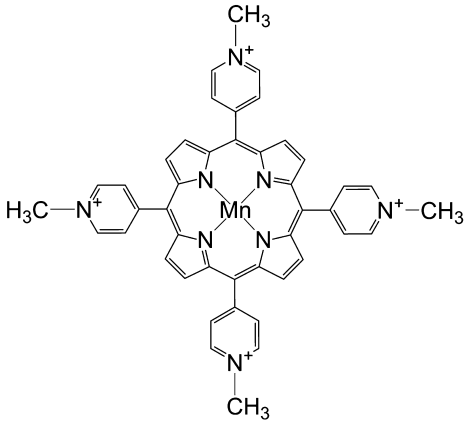

EXPERIMENTAL SECTION

Materials. $Mn^{III}(TMPyP)^{4+}$ was purchased from Porphyrin Products (Logan, UT). Poly[d(A-T)$_2$] and poly[d(G-C)$_2$] were obtained from Sigma-Aldrich. The concentrations of synthetic polynucleotide and $Mn^{III}(TMPyP)^{4+}$ were determined spectrophotometrically using the extinction coefficients: ε_{262nm} = 6600 M^{-1} cm^{-1} and ε_{254nm} = 8400 M^{-1} cm^{-1} for poly[d(A-T)$_2$] and poly[d(G-C)$_2$], respectively. In the $Mn^{III}(TMPyP)^{4+}$ case, two coefficients, namely ε_{463nm} = 93 000 and 130 000 M^{-1} cm^{-1}, have been reported,[28,29] and the latter value was confirmed correct. Aliquots of concentrated $Mn^{III}(TMPyP)^{4+}$ solution were added to a 200 μM polynucleotide solution (typically few microliters to 3 mL of polynucleotide solution) for the absorption and CD measurements, and appropriate corrections were made for the volume change. In steady-state and transient spectroscopic studies, the concentrations of poly[d(A-T)$_2$] and poly[(dG-dC)$_2$] were ca. 20 μM and the base pairs/porphyrin ratio was ~20. The porphyrin stock solution in the phosphate buffer was added to the DNA solution and allowed to stand for 30 min before the spectral measurements. All measurements were performed in 5 mM phosphate buffer at pH 7 containing 100 mM NaCl.

Measurements. The transient resonance Raman (RR) measurement setup is described in detail elsewhere.[30] The transient RR spectra were obtained by photoexcitation with 416 nm pulses, generated by the hydrogen Raman shift of the third harmonic (355 nm) from a nanosecond Q-switched Nd:YAG laser (Continuum, Surelite II, pulse width of ~5 ns (fwhm)). The sample solution was passed through a glass capillary tube at a rate sufficient to ensure that each laser pulse encountered a fresh volume of sample. The Raman spectra were collected using a monochromator (DongWoo Optron, Monora 500i) equipped with an ICCD camera (Andor, iStar). One-color transient Raman spectra were obtained by the difference spectrum between the intense (ca. 0.2 mJ/pulse) and weak (ca. 0.01 mJ/pulse) laser pulse excitations. The spectral features of the ground-state porphyrins were subtracted to yield the excited-state Raman spectra, using a subtraction factor sufficient to avoid negative features.

Nanosecond transient absorption measurements were carried out using the laser flash photolysis technique.[31] The output of the third harmonic generation (355 nm) from a Q-switched Nd:YAG laser was converted to 460 nm pulses by the OPO system (Surelite OPO Plus) to excite the samples. A xenon lamp (ILC Technology, PS 300-1) was focused into the sample solution as the probe light for the transient absorption measurements. The transient absorption spectra were measured using an ICCD camera. The temporal profiles were measured with a monochromator equipped with a photomultiplier (Zolix Instruments Co., CR 131) and a digital oscilloscope (Tektronix, TDS-784D). The reported signals were the mean of 200 events. All solutions were argon-saturated unless indicated otherwise.

The subpicosecond time-resolved absorption spectra were collected using a pump–probe transient absorption spectroscopy system (Ultrafast Systems, Helios).[32] The pump light was generated using a regeneratively amplified titanium sapphire laser system (Coherent, Libra-F, 1 kHz) pumped with a diode-pumped Q-switched laser (Coherent, Evolution). The seed pulse was generated using a titanium sapphire laser (Coherent, Vitesse). The excitation (pump) light at 460 nm was by fourth harmonic generation of the 1840 nm idler beam from an optical parametric amplifier (OPA, Coherent, TOPAS) pumped by the 800 nm fundamental of the amplified laser. A white-light continuum pulse, which was generated by focusing the residual of the fundamental light on a thin CaF_2 crystal after a computer-controlled optical delay, was used as the probe beam. This beam was directed to the sample cell with a 1.0 mm optical path and detected with a CCD detector installed in the absorption spectrometer. The pump pulse was chopped with a mechanical chopper synchronized to one-half of the laser repetition rate, resulting in a pair of spectra with and without the pump from which the absorption change induced by the pump pulse was estimated.

The absorption and CD spectra were recorded on a Cary 100 spectrophotometer (Palo Alto, CA) and Jasco J-810 spectropolarimeter, respectively.

RESULTS AND DISCUSSION

Binding Mode of $Mn^{III}(TMPyP)^{4+}$ to Synthetic Polynucleotides. Figure 1a,b shows the absorption and CD spectrum of $Mn^{III}(TMPyP)^{4+}$ in the Soret absorption region, respectively. A maximum at 462 nm was apparent for $Mn^{III}(TMPyP)^{4+}$ in the absence of a polynucleotide. The absorbance increased by ~39% and the maximum shifted slightly (~1 nm) to a longer wavelength by upon binding to poly[d(A-T)$_2$]. On the other hand, the absorption band became broadened whereas absorbance and maximum wavelength remained when bound to poly[d(G-C)$_2$]. The $Mn^{III}(TMPyP)^{4+}$–poly[d(G-C)$_2$] complex produced a positive CD band at 466 nm in the Soret region, which excluded the possibility of intercalative binding mode, and suggested that it probably binds outside of poly[d(G-C)$_2$]. The two positive CD bands at 461 and 472 nm were apparent when $Mn^{III}(TMPyP)^{4+}$ formed a complex with poly[d(A-T)$_2$]. One of the possibilities of dual-positive CD bands observed for the $Mn^{III}(TMPyP)^{4+}$–poly[d(A-T)$_2$] complex is that the interactions of the two electric transition moments of porphyrin with the chirally arranged DNA bases are different, resulting in a transition that produces a positive band at slightly different

dx.doi.org/10.1021/jp4027699 | J. Phys. Chem. B 2013, 117, 9585–9590

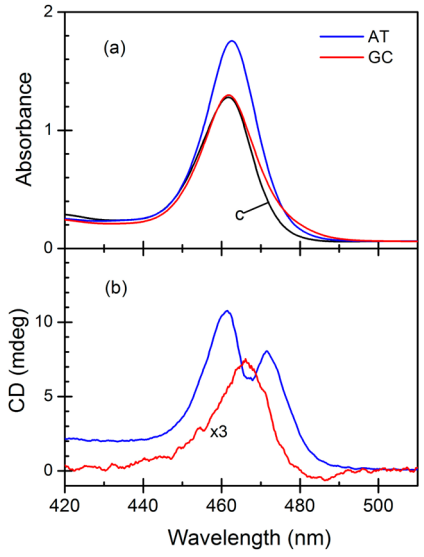

Figure 1. Absorption (a) and CD spectrum (b) of $Mn^{III}(TMPyP)^{4+}$ complexed with poly[d(G-C)$_2$] (red curve, denoted by GC) and poly[d(A-T)$_2$] (blue curve, denoted by AT). The absorption spectrum of polynucleotide-free $Mn^{III}(TMPyP)^{4+}$ (denoted as curve c) is also shown in panel a. CD spectrum of the $Mn^{III}(TMPyP)^{4+}$-poly[d(G-C)$_2$] complex is enlarged three times for easy comparison. [polynucleotide] = 200 μM and [porphyrin] = 10 μM.

wavelengths. Another possibility is the coupling of electric transition moment between DNA-bound porphyrins. A similar CD spectrum was reported in the $Mn^{III}(TMPyP)^{4+}$–native DNA complex case.[20] A positive CD spectrum was produced at a low [porphyrin]/[DNA] ratio, suggesting that porphyrin binds at exterior of the DNA. As the porphyrin density increased, two positive CD bands were observed, which was similar to that observed for the $Mn^{III}(TMPyP)^{4+}$–poly[d(A-T)$_2$] complex (Figure 1b). The fact that the dual positive CD spectrum began to appear with increasing porphyrin density supports the coupling of the electric transition moment between the poly[d(A-T)$_2$]-bound porphyrins. Therefore, in the poly[d(A-T)$_2$] case, the bound $Mn^{III}(TMPyP)^{4+}$ conceivably interact with each other. Similar external binding of $Mn^{III}(TMPyP)^{4+}$ to poly[d(A-T)$_2$] and poly[d(G-C)$_2$] was reported.[21] In contrast, a quantitative analysis of CD spectrum revealed that $Mn^{III}(TMPyP)^{4+}$ binds at the major groove of both poly[d(G-C)$_2$] and poly[d(A-T)$_2$] at the [porphyrin]/[DNA] concentration adopted in this study.[23] In any case, $Mn^{III}(TMPyP)^{4+}$ does not intercalate between polynucleotide base pairs and the $\pi-\pi$ interaction between porphyrin and DNA bases are negligible.

Reduction of $Mn^{III}(TMPyP)^{4+}$ Bound to Poly[d(A-T)$_2$] and Poly[d(G-C)$_2$]. The ground-state Raman spectra of cationic $Mn^{III}(TMPyP)^{4+}$ in a pH 7 aqueous solution, which were recorded using a very low power nanosecond pulse excitation at 416 nm, were assigned readily with reference to the normal-mode analysis of a similar M-$(TMPyP)^{4+}$ (Figure 2A and Table 1).[30,33−35] In an aqueous solution, the ν_2 and ν_4 bands of the porphyrin macrocycle were assigned to 1565 and 1365 cm^{-1}, respectively. *N*-Methylpyridyl bands were also observed: δ(C$_m$-Pyr) at 1251 cm^{-1}, δ(Pyr) at 1220 cm^{-1}, and δ(Pyr) and ν(N$^+$-CH$_3$) at 1194 cm^{-1}. Even when associated with poly[d(G-C)$_2$] or poly[d(A-T)$_2$], most of the Raman bands for ground-state $Mn^{III}(TMPyP)^{4+}$ were indistinguishable from those in the aqueous solution (Figure 2, A(b) and (c)).

Table 1. Raman Frequencies (cm^{-1}) and Band Assignments of $Mn^{III}(TMPyP)^{+4}$ in the Ground and Excited States

assignments	in aqueous solution	poly[d(G-C)$_2$]	poly[d(A-T)$_2$]
ϕ_4, δ(pyr)	1644 (1644)	1644 (1642)	1644 (1640)
ν_2, ν(C$_\beta$C$_\beta$)	1565 (1558)	1563 (1537)	1563 (1536)
ν_3, ν(C$_\alpha$C$_\beta$)	1455 (1452)	1457 (1434)	1455 (1434)
ν_4, ν(C$_\alpha$N)	1365 (1356)	1366 (1343)	1365 (1340)
–	1291	1297	1295
ν_1, δ(C$_m$-pyr)	1251 (1254)	1253 (1251)	1253 (1249)
δ(pyr)		1219 (1217)	1219 (1217)
δ(pyr), ν(N$^+$-CH$_3$)	1184 (1186)	1194 (1188)	1193 (1187)
ν_9, δ(C$_\beta$–H)	–	(1093)	(1093)

[a]Values shown in parentheses were obtained in the excited state.

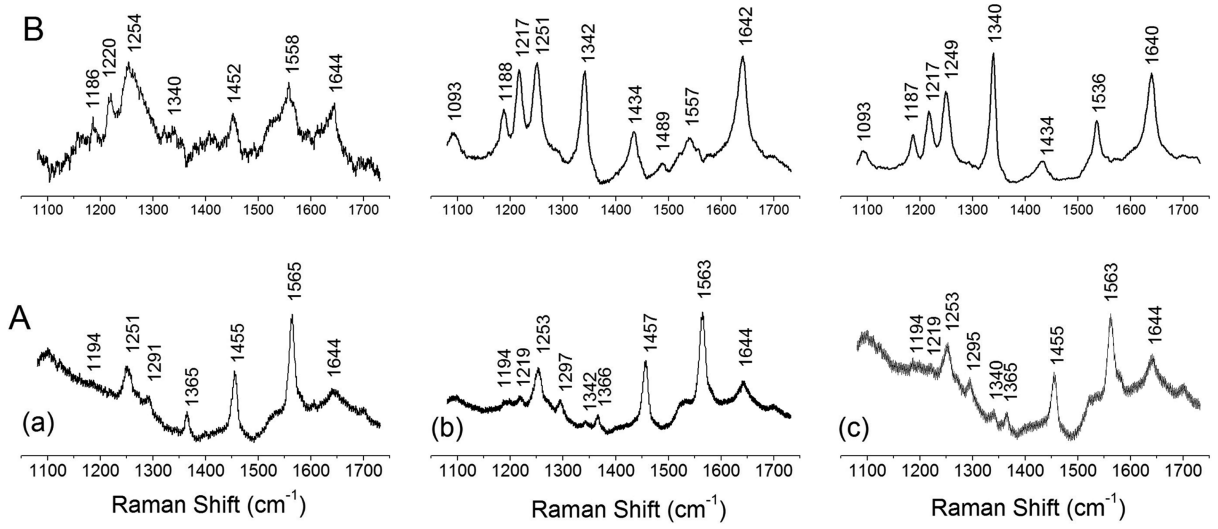

Figure 2. Ground-state Raman spectra of $Mn^{III}(TMPyP)^{4+}$ with a low power (ca. 0.01 mJ/pulse) probe pulses at 416 nm (panel A) and nanosecond transient Raman spectra of $Mn^{III}(TMPyP)^{4+}$ with high power (ca. 0.2 mJ/pulse) pump and probe pulses at 416 nm (panel B) in the phosphate buffer solution (pH 7) (spectrum a), and that bound to poly[d(G-C)$_2$] (spectrum b) and poly[d(A-T)$_2$] (spectrum c).

dx.doi.org/10.1021/jp4027699 | J. Phys. Chem. B 2013, 117, 9585−9590

Figure 2B shows the transient Raman spectrum of $Mn^{III}(TMPyP)^{4+}$ obtained by high-power 416 nm single-pulse excitation. The Raman spectral features for the ground-state $Mn^{III}(TMPyP)^{4+}$ were subtracted to yield an excited-state Raman spectrum using a subtraction factor sufficient to avoid negative features. In an aqueous solution, the core-size sensitive Raman bands at 1558, 1452, and 1340 cm^{-1} were shifted slightly to lower frequencies compared to the ground-state Raman bands (Figure 2B(a)). The *N*-methylpyridyl-related bands were enhanced at 1644, 1254, 1220, and 1186 cm^{-1}, respectively. When bound to poly[d(A-T)$_2$], the characteristic *N*-methylpyridyl bands of the transient Raman spectra at 1251, 1217, and 1188 cm^{-1} were enhanced markedly (Figure 2B(b)). Corresponding enhancement was observed at 1249, 1217, and 1187 cm^{-1} when bound to poly[d(G-C)$_2$] (Figure 2B(c)). The ν_1 mode assigned to C_m-aryl stretching was intense in the transient Raman spectra, which is in parallel with the enhancement of the ν_4 mode. The ν_1 mode has a contribution from the internal *N*-methylpyridyl vibration motion. The enhancement of the internal *N*-methylpyridyl mode (ϕ_4 mode) and ν_1 mode is an essential indicator of porphyrin ring-to-*N*-methylpyridyl charge transfer in the excited state.[36] Furthermore, the enhancement of these modes also reflects the increased π-electron conjugation between the porphyrin plane and peripheral groups, probably induced by the rotation of peripheral groups toward the porphyrin plane in the excited state.[37]

In particular, when bound either to poly[d(A-T)$_2$] or poly[d(G-C)$_2$], large downshifts of ca. 25 cm^{-1} of the ν_2 and ν_4 modes of $Mn^{III}(TMPyP)^{4+}$ were observed in the transient Raman spectra. The ν_2 and ν_4 modes are strongly correlated with the oxidation state, spin state, and core size of metalloporphyrins.[38,39] Because $Mn^{III}(TMPyP)^{4+}$ has a high-spin d^4 configuration, four d-orbitals are singly occupied and only the antibonding $d_{x^2-y^2}$ orbital remains empty. In contrast, photoreduced Mn^{II} porphyrin has a high-spin d^5 configuration. The population of the $d_{x^2-y^2}$ orbital, essentially by antibonding electrons, causes large out-of-plane displacement of the Mn^{II} ion.[38,39] The core size of the macrocycle of $Mn^{II}(TMPyP)^{4+}$ is increased, which does not favor charge-transfer transitions. As a consequence, $Mn^{III}(TMPyP)^{4+}$, in which charge-transfer reaction occurs easily, exhibited the Soret absorption band near ~460 nm which is in contrast with that of 435 nm for $Mn^{II}(TMPyP)^{4+}$.[40,41] These concepts made the spectral changes at ν_2 and ν_4 modes good indicators for determining the redox species of manganese porphyrins. Therefore, the change in the transient Raman spectrum at the ν_2 and ν_4 modes suggests that $Mn^{III}(TMPyP)^{4+}$ is photoreduced to $Mn^{II}(TMPyP)^{4+}$ in the excited state when bound to either poly[d(A-T)$_2$] or poly[d(G-C)$_2$]. Electron transfers easily from the G base forming a radical cation $G^{\bullet+}$ due to the low oxidation potential of the G base. Therefore, the reduction of $Mn^{III}(TMPyP)^{4+}$, which is bound to poly[d(A-T)$_2$], to $Mn^{II}(TMPyP)^{4+}$ is significant because an electron can also transfer from the AT base pairs, probably from the A base, forming the radical cation $A^{\bullet+}$ in the excited state. From the conventional absorption and CD study in the previous section, $Mn^{III}(TMPyP)^{4+}$ appeared to bind the exterior of both poly[d(A-T)$_2$] and poly[d(G-C)$_2$]. Therefore, direct contact of $Mn^{III}(TMPyP)^{4+}$ with the G or A base is not a necessary condition for the electron to transfer. Finally, it is noteworthy that there could be alternative explanation for observed data. The photoreduced species is possibly related to the long-lived (d−d) state of $Mn^{III}(TMPyP)^{4+}$ with a large population at the $d_{x^2-y^2}$ orbital. However, if this is the case, the intrinsic transition is expected to be similar in aqueous solution and when bound to poly[d(G-C)$_2$] or poly[d(A-T)$_2$]. The fact that the transition in the aqueous solution is different from those bound to polynucleotides suggested that the intrinsic transition is conceivably not the case.

Properties of Excited $Mn^{III}(TMPyP)^{4+}$ Bound to Polynucleotides. Figure 3, a and b, shows the femtosecond time-resolved transient absorption (fs-TA) spectra of $Mn^{III}(TMPyP)^{4+}$ upon excitation with a 460 nm femtosecond pulse in the presence and absence of poly[(d(G-C)$_2$]. In both cases, large changes in absorbance were observed at 430 and 500 nm immediately after excitation. The rapid decay in absorbance was also common for both cases. On the other hand, there were differences in the decay profile. In the absence of a polynucleotide, the absorbance at 430 nm decays in the single-exponential manner. The decay time was 1.3 ps (Figure 3a, inset). Similar decay of 1.4 ps was observed at 480 nm (data not shown). The absorbance of $Mn^{III}(TMPyP)^{4+}$ associated with poly[d(G-C)$_2$] at 500 nm also decayed with a single decay time of 1.0 ps (data not shown). In addition to the presence of a rapid decay time of 0.9 ps, which is similar to that observed at 500 nm, a long component was observed at 430 nm (Figure 3b, inset). The decay times of the nanosecond transient absorption (ns-TA) of $Mn^{III}(TMPyP)^{4+}$ in the presence and absence of polynucleotides in the nanosecond range were also measured. In the absence of polynucleotide, $Mn^{III}(TMPyP)^{4+}$ did not produce any long-lived decay in the entire wavelength range. That measured at 480 nm is shown at the bottom of Figure 4 as an example. When it was associated with poly[d(G-C)$_2$],

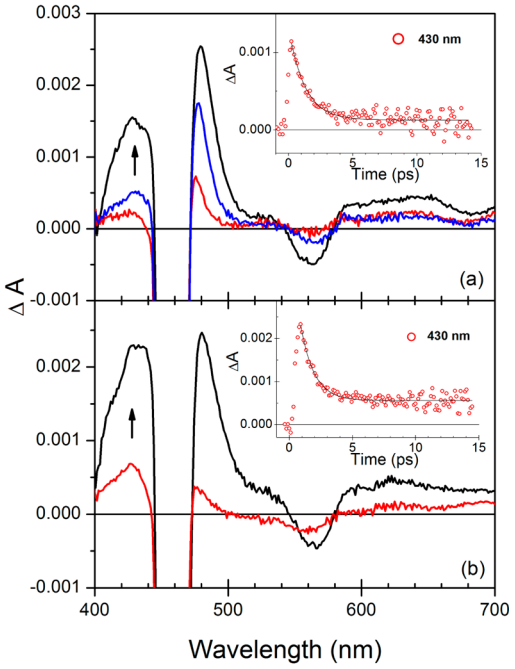

Figure 3. Transient absorption spectra of polynucleotide-free $Mn^{III}(TMPyP)^{4+}$ (panel a) and that bound to poly[d(G-C)$_2$] (panel b). The spectra were measured at a delay time of 0.8, 1.4, and 3.6 ps (to the direction of arrow) in panel a and of 0.8 and 5.8 ps in panel b. The excitation wavelength was 460 nm (fwhm = ~130 fs). The decay profiles (inset) were monitored at 430 nm for both in the presence and absence of poly[d(G-C)$_2$].

dx.doi.org/10.1021/jp4027699 | J. Phys. Chem. B 2013, 117, 9585−9590

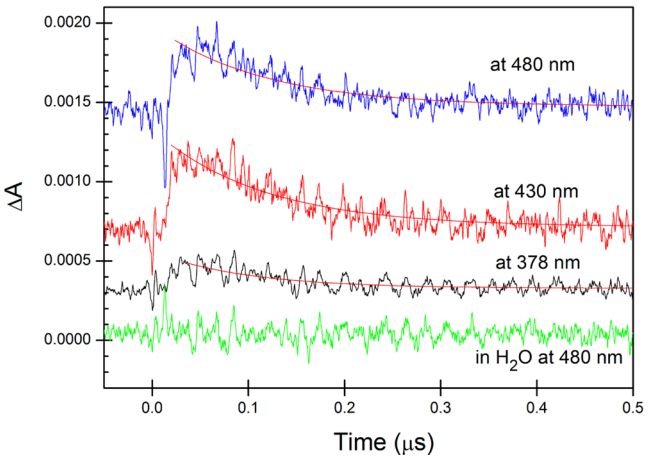

Figure 4. Decay profiles of the $Mn^{III}(TMPyP)^{4+}$–poly[d(G-C)$_2$] adduct measured at the wavelengths of 378, 430, and 480 nm in the nanosecond time scale. That at 480 nm in the absence of polynucleotide is also shown at the bottom (green curve).

$Mn^{III}(TMPyP)^{4+}$ exhibited a long-lived decay in ns-TA spectrum as shown in Figure 4. The decay times measured at 378, 430, and 480 nm were 115 ns (Figure 4). The shorter component of the fs-TA bands can be assigned to the S_1–S_n transition for $Mn^{III}(TMPyP)^{4+}$. The long component conceivably corresponds to the oxidation of photoinduced $Mn^{II}(TMPyP)^{4+}$ species, whose electron originates from the G base. A similar change in the fs-TA spectrum was observed for the adduct formed between $Mn^{III}(TMPyP)^{4+}$ and poly[d(A-T)$_2$]: the short decay time was 1.1 and 0.9 ps at 500 and 430 nm, respectively (Figure S1 in the Supporting Information). Similarly, with the $Mn^{III}(TMPyP)^{4+}$–poly[d(G-C)$_2$] adduct, the decay did not reach zero in the $Mn^{III}(TMPyP)^{4+}$–poly[d(A-T)$_2$] adduct case, suggesting also the presence of a long decay component. Indeed, the decay times of 65 ns were observed at 378, 400, and 490 nm (Figure S2 in the Supporting Information) using the ns-TA measurement. This suggests that the oxidation of $Mn^{II}(TMPyP)^{4+}$ occurred even at the AT base pair.

ΔG_{PET}, which is the free energy of photoinduced electron transfer, of the excited state was evaluated using the following equation

$$\Delta G_{PET} = (E^0_{ox} - E^0_{red}) - E_{00}$$

where E^0_{ox} and E^0_{red} are the oxidation and reduction potentials for the donor (A or G) and acceptor ($Mn^{III}(TMPyP)^{4+}$) molecules, respectively, and E_{00} denotes the excitation energy. The ΔG_{PET} values can be estimated from the reported reduction potential of $Mn^{III}(TMPyP)^{4+}$ (−0.15 V vs SCE) and the oxidation potentials of the G and A bases (1.24 and 1.69 V vs SCE).[42,43] The excitation energy of $Mn^{III}(TMPyP)^{4+}$ was determined to be 1.98 eV from the end point of the Q-band of $Mn^{III}(TMPyP)^{4+}$. The resulting ΔG_{PET} values for photoinduced electron transfer from G or A to $Mn^{III}(TMPyP)^{4+}$ were negative as shown in Table 2. The negative ΔG_{PET} suggests that photoinduced electron transfer can occur spontaneously for both poly[d(A-T)$_2$] and poly[d(G-C)$_2$], producing $Mn^{II}(TMPyP)^{4+}$–poly[d($G^{\bullet+}$-C)$_2$] and the $Mn^{II}(TMPyP)^{4+}$–poly[d($A^{\bullet+}$-C)$_2$] radical species, suggesting the formation of a hole at the G or A base.

Table 2. Reduction Potential of $Mn^{III}(TMPyP)^{+4}$ and Oxidation Potential of DNA Bases (E_{ox} and E_{red} in V vs SCE)

$E_{red}(Mn^{III}P)$	E_{ox}(G)	E_{ox}(A)	E_{00}, eV	ΔG_{PET}, eV
−0.15	1.24		1.98	−0.59
−0.15		1.69	1.98	−0.14

CONCLUSIONS

The transient Raman and transient absorption spectral features of the poly[d(A-T)$_2$]– and poly[d(G-C)$_2$]–$Mn^{III}(TMPyP)^{4+}$ complexes were in good agreement with the characteristics of reduced Mn^{II} porphyrins, suggesting that $Mn^{III}(TMPyP)^{4+}$ can be reduced when bound to both poly[d(A-T)$_2$] and poly[d(G-C)$_2$] in the excited state. This suggests that both polynucleotides act as electron donors and that both polynucleotides are photo-oxidized in the excited state. This highlights the possibility of hole formation at the AT base pair in addition to the well-known hole formation at the GC site, and will help better understand other photoreactions of DNA using Mn^{III} porphyrins.

ASSOCIATED CONTENT

Supporting Information

Transient absorption spectra of $Mn^{III}(TMPyP)^{4+}$ in poly[d(A-T)$_2$] measured at delay times of 0.7 and 7.2 ps, and decay profiles of the $Mn^{III}(TMPyP)^{4+}$–poly[d(A-T)$_2$] adduct. This material is available free of charge via the Internet at http://pubs.acs.org.

AUTHOR INFORMATION

Corresponding Author

*E-mail: dwcho@korea.ac.kr (D.W.C.); seogkim@yu.ac.kr (S.K.K.) Tel.: + 82 53 810 2362. Fax: +82 53 815 5412.

Notes

The authors declare no competing financial interest.

ACKNOWLEDGMENTS

This study was supported by the Korean Research Foundation (Grant no. 2012-008875) conferred to S.K.K. and by the Seoul R&BD program (WR090671) to C.I.

REFERENCES

(1) Matts, P. J.; Fink, B. Chronic Sun Damage and the Perception of Age, Health and Attractiveness. *Photochem. Photobiol. Sci.* **2010**, *9*, 421–431.

(2) Foster, K. W.; Katiyar, S. K.; Yusuf, N.; Elmets, C. A. *Biophysical and Physiological Effects of Solar Radiation on Human Skin*; Giacomoni, P. U., Ed.; The Royal Society of Chemistry: London, 2007; pp 25–63.

(3) Panelos, J.; Tarantini, F.; Paglierani, M.; Serio, C. D.; Maio, V.; Pellerito, S.; Pimpinelli, N.; Santucci, M.; Massi, D. Photoexposition Discriminates Notch 1 Expression in Human Cutaneous Squamous Cell carcinoma. *Mod. Pathol.* **2008**, *21*, 316–325.

(4) Kawai, K.; Takada, T.; Nagai, T.; Cai, X.; Sugimoto, A.; Fujitsuka, M.; Majima, T. Long-Lived Charge-Separated State Leading to DNA Damage through Hole Transfer. *J. Am. Chem. Soc.* **2003**, *125*, 16198–16199.

(5) Takada, T.; Kawai, K.; Fujitsuka, M.; Majima, T. Direct Observation of Hole Transfer through Double-helical DNA over 100 Å. *Proc. Natl. Acad. Sci. U.S.A* **2004**, *101*, 14002–14006.

(6) Dohno, C.; Nakatani, K.; Saito, I. Guanine of the Third Strand of C·G*G Triplex Serves as an Effective Hole Trap. *J. Am. Chem. Soc.* **2002**, *124*, 14580–14585.

(7) Daublain, P.; Siegmund, K.; Hariharan, M.; Vura-Weis, J.; Wasielewski, M. R.; Lewis, F. D.; Shafirovich, V.; Wang, Q.; Raytchev,

M.; Fiebig, T. Photoinduced Charge Separation in Pyrenedicarboxamide-Linked DNA Hairpins. *Photochem. Photobiol. Sci.* **2008**, *7*, 1501−1508.
(8) Fiel, R. J. Porphyrin-Nucleic Acid Interactions: A Review. *J. Biomol. Struct. Dyn.* **1989**, *6*, 1259−1274.
(9) Fiel, R. J.; Howard, J. C.; Mark, E. H.; Datta-Gupta, N. Interaction of DNA with a Porphyrin Ligand: Evidence for Intercalation. *Nucleic Acids Res.* **1979**, *6*, 3093−3118.
(10) Pasternack, R. F.; Bustamante, C.; Collings, P. J.; Giannetto, A.; Gibbs, E. J. Porphyrin Assemblies on DNA as Studied by a Resonance Light-Scattering Technique. *J. Am. Chem. Soc.* **1993**, *115*, 5393−5399.
(11) Pasternack, R. F.; Ewen, S.; Rao, A.; Meyer, A. S.; Freedman, M. A.; Collings, P. J.; Frey, S. L.; Ranen, M. C.; de Paula, J. C. Interactions of Copper(II) Porphyrins with DNA. *Inorg. Chim. Acta* **2001**, *317*, 59−71.
(12) Pasternack, R. F.; Giannetto, A.; Pagano, P.; Gibbs, E. J. Self-Assembly of Porphyrins on Nucleic Acids and Polypeptides. *J. Am. Chem. Soc.* **1991**, *113*, 7799−7800.
(13) Sessler, J. L.; Cyr, M. J.; Lynch, V.; McGhee, E.; Ibers, J. A. Synthetic and Structural Studies of Sapphyrin, a 22-π-electron Pentapyrrolic "Expanded Porphyrin". *J. Am. Chem. Soc.* **1990**, *112*, 2810−2813.
(14) Moore, C. M.; Pendse, D.; Emberton, M. Photodynamic Therapy for Prostate Cancer-A Review of Current Status and Future Promise. *Nat. Clin. Pract. Urol.* **2009**, *6*, 18−30.
(15) Marzilli, L. G.; Banville, D. L.; Zon, G.; Wilson, W. D. Pronounced Proton and Phosphorus-31 NMR Spectral Changes on *meso*-Tetrakis(N-methylpyridinium-4-yl)porphyrin Binding to Poly[d-(G-C)]·poly[d(G-C)] and to Three Tetradecaoligodeoxyribonucleotides: Evidence for Symmetric, Selective Binding to 5′CG3′ Sequences. *J. Am. Chem. Soc.* **1986**, *108*, 4188−4192.
(16) Guliaev, A. B.; Leontis, N. B. Cationic 5,10,15,20-Tetrakis(*N*-methylpyridinium-4-yl)porphyrin Fully Intercalates at 5′-CG-3′ Steps of Duplex DNA in Solution. *Biochemistry* **1999**, *38*, 15425−15437.
(17) Fedoroff, O. Y.; Rangan, A.; Chemeris, V. V.; Hurley, L. H. Cationic Porphyrins Promote the Formation of i-Motif DNA and Bind Peripherally by a Nonintercalative Mechanism. *Biochemistry* **2000**, *39*, 15083−15090.
(18) Kelly, J. M.; Murphy, M. J.; McConnell, D. J.; OhUigin, C. A Comparative Study of the Interaction of 5,10,15,20-tetrakis(N-methylpyridinium-4-yl)porphyrin and Its Zinc Complex with DNA Using Fluorescence Spectroscopy and Topoisomerisation. *Nucleic Acids Res.* **1985**, *13*, 167−184.
(19) Pasternack, R. F. Circular Dichroism and the Interactions of Water Soluble Porphyrins with DNA-A Minireview. *Chirality* **2003**, *15*, 329−332.
(20) Gong, L.; Bae, I.; Kim, S. K. Effect of Axial Ligand on the Binding Mode of M-*meso*-Tetrakis(*N*-methylpyridinium-4-yl)-porphyrin to DNA Probed by Circular and Linear Dichroism Spectroscopies. *J. Phys. Chem. B* **2012**, *116*, 12510−12521.
(21) Pasternack, R. F.; Gibbs, E. J.; Villafranca, J. J. Interactions of Porphyrins with Nucleic Acids. *Biochemistry* **1983**, *22*, 2406−2414.
(22) Kuroda, R.; Tanaka, H. J. DNA-porphyrin Interactions Probed by Induced CD Spectroscopy *Chem. Soc. Chem. Commun.* **1994**, 1575−1576.
(23) Nitta, Y.; Kuroda, R. Quantitative Analysis of DNA-porphyrin Interactions. *Biopolymers* **2006**, *81*, 376−391.
(24) Kruglik, S. G.; Mojzes, P.; Mizutani, Y.; Kitagawa, T.; Turpin, P-.Y. Time-Resolved Resonance Raman Study of the Exciplex Formed between Excited Cu-Porphyrin and DNA. *J. Phys. Chem. B* **2001**, *105*, 5018−5031.
(25) Jeoung, S. C.; Eom, H. S.; Kim, D.; Cho, D. W.; Yoon, M. Exciplex Formation Dynamics of Photoexcited Copper(II) Tetrakis(4-*N*-methylpyridyl)porphyrin with Synthetic Polynucleotides Probed by Transient Absorption and Raman Spectroscopic Techniques. *J. Phys. Chem. A* **1997**, *101*, 5412−5417.
(26) Gouterman, M. In *The Porphyrins*; Dolphin, D., Ed.; Academic Press: New York, 1978; Vol. *III*.
(27) Suslick, K. S.; Watson, R. A. The Photochemistry of Chromium, Manganese, and Iron Porphyrin complexes. *New. J. Chem.* **1992**, *16*, 633−642.
(28) Harriman, A.; Porter, G. Photochemistry of Manganese Porphyrins. Part 1.-Characterisation of Some Water Soluble Complexes. *J. Chem. Soc., Faraday Trans. 2* **1979**, *75*, 1532−1542.
(29) Batinić-Haberle, I.; Benov, L.; Spasojević, I.; Fridovich, I. The *Ortho* Effect Makes Manganese(III)*Meso*-Tetrakis(*N*-Methylpyridinium-2-yl)Porphyrin a Powerful and Potentially Useful Superoxide Dismutase Mimic. *J. Biol. Chem.* **1998**, *273*, 24521−24528.
(30) Cho, D. W.; Jeong, D. H.; Ko, J-.H.; Kim, S. K.; Yoon, M. Raman Spectroscopic Studies on Interactions of Water Soluble Cationic Oxovanadyl (IV) *meso*-tetrakis(1-methylpyridium-4-yl) porphyrin with Nucleic Acids. *J. Photochem. Photobiol. A: Chem.* **2005**, *174*, 207−213.
(31) Cho, D. W.; Fujitsuka, M.; Ryu, J. H.; Lee, M. H.; Kim, H. K.; Majima, T.; Im, C. S_2 Emission from Chemically Modified BODIPYs. *Chem. Commun.* **2012**, *48*, 3424−3426.
(32) Cho, D. W.; Cho, D. W.; Park, H. J.; Yoon, U. C.; Lee, M. H.; Im, C. Synergistic Effect of Ttrimethylsilane for Photoinduced Electron Transfer on 1,8-Naphthalimides in Polar Solvent. *J. Photochem. Photobiol. A: Chem.* **2012**, *246*, 23−28.
(33) Blom, N.; Odo, J.; Nakamoto, K.; Strommen, D. P. Resonance Raman Studies of Metal tetrakis(4-N-methylpyridyl)porphine: Band Assignments, Structure-sensitive Bands, and Species Equilibria. *J. Phys. Chem.* **1986**, *90*, 2847−2852.
(34) Ha, J.-S.; Song, O.-K.; Yoon, M.; Kim, D. Surface-induced Substitution Reaction on Cobalt(III) and Manganese(III) Tetrakis(4-*N*-methylpyridyl)porphyrins Probed by Surface-enhanced Raman Spectroscopy. *J. Raman Spectrosc.* **1990**, *21*, 667−674.
(35) Song, O.-K.; Yoon, M.; Kim, D. Surface-enhanced Raman Scattering of Zinc Tetrakis(4-*N*-methylpyridyl)porphyrin. *J. Raman Spectrosc.* **1989**, *20*, 739−743.
(36) Jeoung, S. C.; Kim, D.; Cho, D. W.; Yoon, M. Time-Resolved Resonance Raman Spectroscopic Study on Metallo-tetraphenylporphyrins: Effect of Metal Sizes. *Bull. Korean Chem. Soc.* **1999**, *20*, 657−662.
(37) Jeoung, S. C.; Kim, D.; Ahn, K-.H.; Cho, D. W.; Yoon, M. Time-Resolved Resonance Raman Spectra of Free-base Tetraarylporphyrins: Effects of the Peripheral Substituents. *Chem. Phys. Lett.* **1995**, *241*, 533−539.
(38) Jeoung, S. C.; Kim, D.; Cho, D. W. Transient Resonance Raman Spectroscopic Studies of Some Paramagnetic Metalloporphyrins: Effects of Axial Ligand on Charge-transfer and Photoreduction Processes. *J. Raman Spectrosc.* **2000**, *31*, 319−330.
(39) Jeoung, S. C.; Kim, D.; Cho, D. W.; Yoon, M. Transient Absorption and Resonance Raman Investigations on the Axial Ligand Photodissociation of Halochromium(III) Tetraphenylporphyrin. *J. Phys. Chem. A* **2000**, *104*, 4816−4824.
(40) Morehouse, K. M.; Neta, P. Kinetics of Demetalation of Manganese(II) Porphyrins in Aqueous Solutions. *J. Phys. Chem.* **1984**, *88*, 3118−3120.
(41) Morehouse, K. M.; Neta, P. Redox Reactions of Manganese Porphyrins in Aqueous Solutions. Steady-state and Pulse Radiolysis Spectrophotometric Studies. *J. Phys. Chem.* **1984**, *88*, 1575−1579.
(42) Yu, C-.H.; Su, Y. O. Electrocatalytic Reduction of Nitric Oxide by Water-Soluble Manganese Porphyrins. *J. Electroanal. Chem.* **1994**, *368*, 323−327.
(43) Seidel, C. A. M.; Schulz, A.; Sauer, M. H. Nucleobase-Specific Quenching of Fluorescent Dyes. 1. Nucleobase One-Electron Redox Potentials and Their Correlation with Static and Dynamic Quenching Efficiencies. *J. Phys. Chem.* **1996**, *100*, 5541−5553.